

Electronic Supplementary Information

Synthesis, crystal structure of the simultaneous binding of Ni(II) cation and chloride by the protonated 2,4,6 tris-(2-pyridyl)-1,3,5 triazine ligand: Theoretical investigations of anion $\cdots\pi$, $\pi\cdots\pi$ and hydrogen bonding interactions

Pampi Pal,^a Kinsuk Das^{*,b}, Anowar Hossain,^a Rosa M. Gomila^c, Antonio Frontera^{*,d}, and Subrata Mukhopadhyay^{*,a}

^a*Department of Chemistry, Jadavpur University, Kolkata 700032, India*

^b*Department of Chemistry, Chandernagore College, Hooghly, West Bengal 712136, India*

^c*Serveis Científic-Tècnics, Universitat de les IllesBalears, Crta. de Valldemossa km 7.5, Palma 07122, Balears, Spain*

^d*Departament de Química, Universitat de les IllesBalears, Crta. de Valldemossa km 7.5, Palma 07122, Balears, Spain*

Contents of the Supporting Information

Table S1	Selected crystallographic features of structure 1	Page S2
Table S2	Coordination bond distances (Å) and angles (°) for 1	Page S3
Table S3	Details of Hydrogen bond distances (Å) and angles (°) for 1	Page S3
Table S4	Geometric features (distances in Å and angles in degrees) of $\pi\cdots\pi$ interactions obtained for 1	Page S4
Scheme S1	Schematic representation of the possible coordination modes of the ligand ' tptz '	Page S5
Scheme S2	[a] Availability and the nature of coronation pockets in tptz [b] Schematic representation of steric constrain of the protonated ligand (Htptz ⁺) executed by the hydrogen atoms on the approach of second metal ion (M2) when it is already coordinated to the first metal ion (M1)	Page S5
Scheme S3	Schematic representation of the synthesis of complex 1	Page S6
Figure S1	IR spectrum for Complex 1	Page S6
Figure S2	UV-Visible spectrum for Complex 1	Page S7
Figure S3	TG curve for complex 1	Page S7

Table S1. Selected crystallographic features of structure **1**

Compound	1
Empirical formula	$C_{18}H_{21}Cl_3N_6NiO_4$
Formula weight	550.47
Temperature (K)	150 (2) K
Wavelength (Å)	0.71073
Crystal system	Monoclinic
Space group	P 2 ₁ /n
Unit cell dimensions	
a (Å)	12.5147(10)
b (Å)	14.4871(13)
c (Å)	13.4749(11)
α (°)	90
β (°)	107.825(2)
γ (°)	90
Volume (Å ³)	2325.7(3)
Crystal size (mm ³)	0.10x0.11x0.13
z	4
Density _{cal} (Mgm ⁻³)	1.572
Absorption coefficient (mm ⁻¹)	1.216
F(000)	1128
θ Range (°) for data collection	2.1 – 27.1
Index ranges	-16 ≤ h ≤ 16 -18 ≤ k ≤ 18 -17 ≤ l ≤ 17
Goodness-of-fit on F ²	1.049
Independent reflections [R _{int}]	5038 (0.0407)
Absorption correction	Multi-scan
Refinement method	Full-matrix least squares on F ²
Data/restraints/parameters	5038/ 0/ 325
Reflections collected	34100
Final R indices[I > 2σ (I)]	R=0.0246 wR ₂ =0.0591
Largest difference peak & hole(eÅ ⁻³)	-0.317, 0.292

Table S2. Coordination bond distances (Å) and angles (°) for **1**

Selected Bonds	Value (Å)	Selected Angles	(°)
Ni1 - N1	2.1486(12)	N1 - Ni1 - N2	76.62(4)
Ni1 - N2	2.0010(11)	N2 - Ni1 - N3	75.96(5)
Ni1 - N3	2.1721(12)	N1 - Ni1 - O1	85.35(5)
Ni1 - O1	2.0726(13)	N1 - Ni1 - O2	88.69(5)
Ni1 - O2	2.0822(12)	N1 - Ni1 - Cl1	106.6(3)
Ni1 - Cl1	2.3072(4)	N2 - Ni1 - O1	91.88(5)
		N2 - Ni1 - Cl1	176.55(4)
		N2 - Ni1 - O2	91.15(5)
		N3 - Ni1 - O1	94.38(6)
		N3 - Ni1 - O2	93.00(5)
		N3 - Ni1 - Cl1	100.83(3)
		N1 - Ni1 - N3	152.56(5)
		O1 - Ni1 - O2	172.51(5)
		O1 - Ni1 - Cl1	89.64(4)
		Cl1 - Ni1 - O2	87.72(4)

Table S3. Details of Hydrogen bond distances (Å) and angles (°) for **1**

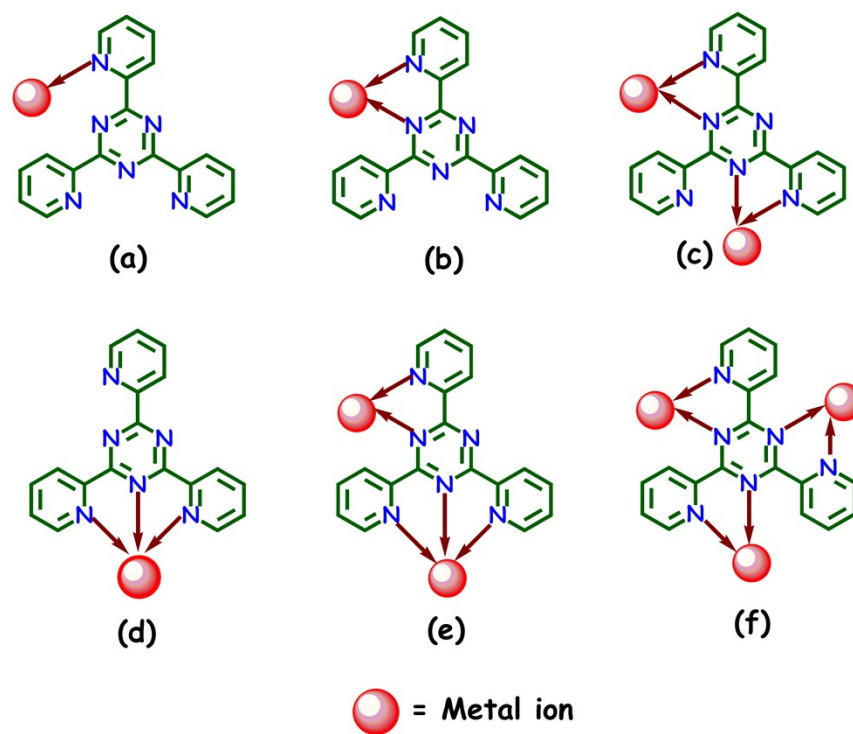
D - H ... A	D (D - H)	D (HA)	D(D...A)	<DHA
N6-H5...Cl2	0.90(2)	2.32(2)	3.1405(15)	152.1(19)
O1-H19...Cl2	0.84(2)	2.26(2)	3.0833(14)	166(2)
O1-H20...Cl1	0.84(2)	2.26(2)	3.0980(14)	173.2(19)
O2-H21...O4	0.82(2)	1.88(2)	2.694(2)	171(2)
O2-H22...Cl3	0.80(2)	2.28(2)	3.0721(14)	175(2)
O3-H23...Cl3	0.75(2)	2.49(2)	3.232(2)	169(2)
O3-H24...Cl2	0.75(3)	2.39(3)	3.133(2)	171(3)
O4-H25...O3	0.89(3)	1.99(3)	2.837(3)	159(3)
O4-H26...Cl3	0.73(3)	2.39(3)	3.1020(17)	165(2)
C2-H2...Cl2	0.9500	2.8200	3.6237(19)	143
C3-H3...Cl1	0.9500	2.6000	3.4598(18)	150
C4-H4...Cl2	0.9500	2.6600	3.6126(17)	177

Table S4. Geometric features (distances in Å and angles in degrees) of $\pi\cdots\pi$ interactions obtained for **1**

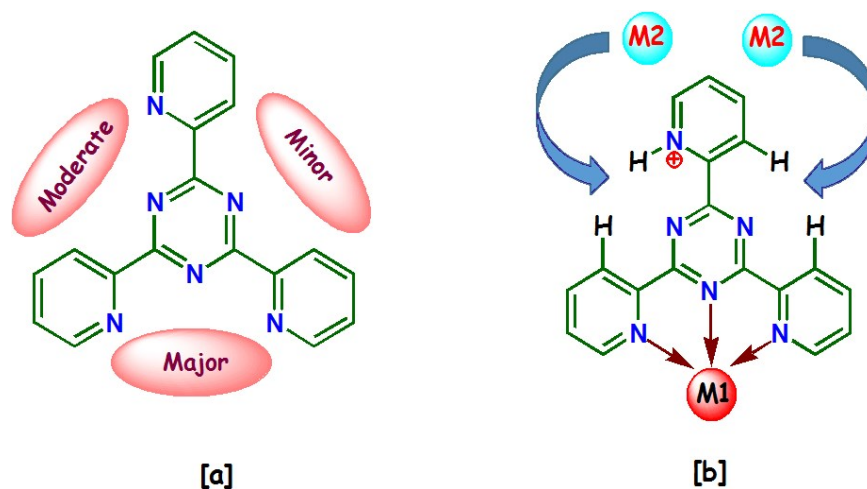
Cg(ring I) - Cg(ring J)	Cg\cdotsCg (Å)	Cg(I) \cdotsperp (Å)	Cg(J) \cdotsperp (Å)	α (°)	β (°)	γ (°)	Symmetry
Cg(3) \cdots Cg(5)	3.6757(9)	3.3674(6)	3.4849(6)	5.11(8)	18.5	23.6	$\frac{1}{2}+x, \frac{3}{2}-y, \frac{1}{2}+z$
Cg(3) \cdots Cg(6)	3.8936(10)	3.5380(6)	3.3513(7)	6.84(8)	30.6	24.7	1-x, 1-y, 1-z
Cg(5) \cdots Cg(3)	3.6757(9)	3.4850(6)	3.3673(6)	5.11(8)	23.6	18.5	$-\frac{1}{2}+x, \frac{3}{2}-y, -\frac{1}{2}+z$
Cg(6) \cdots Cg(3)	3.8939(10)	3.3515(7)	3.5381(6)	6.84(8)	24.7	30.6	1-x, 1-y, 1-z

α = Dihedral angle between ring I and ring J (°); β = Cg(I) \rightarrow Cg(J) or Cg(I) \rightarrow Me vector and normal to plane I (°); γ = Cg(I) \rightarrow Cg(J) vector and normal to plane J (°); Cg–Cg = distance between ring centroids (Å); CgI \cdots Perp = perpendicular distance of Cg(I) on ring J (Å); CgJ \cdots Perp = perpendicular distance of Cg(J) on ring I (Å).

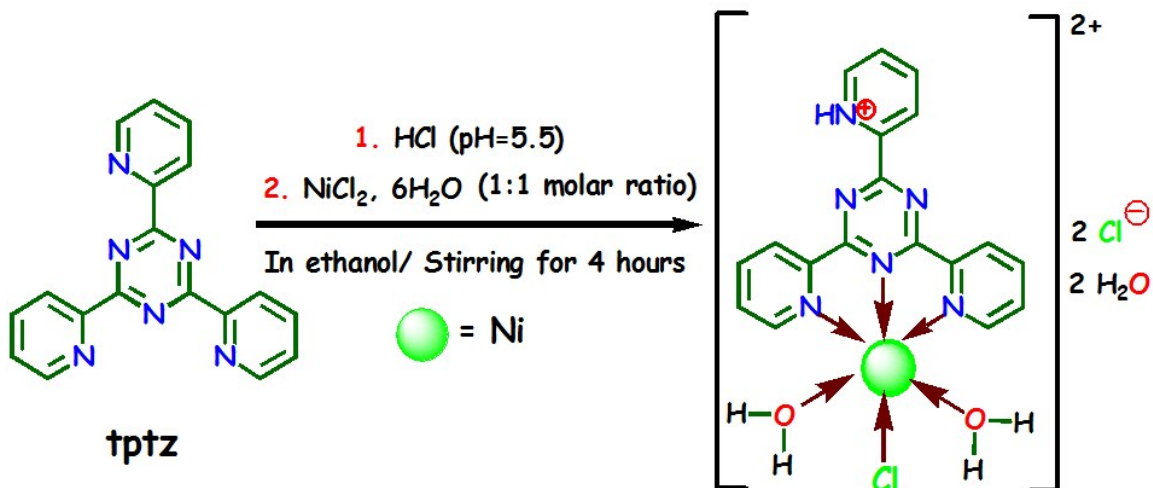
Cg(3) = Centre of gravity of ring [N1/C1/C2/C3/C4/C5], Cg(5) = Centre of gravity of ring [N3/C14/C15/C16/C17/C18] and Cg(6) = Centre of gravity of ring [N6/C8/C9/C10/C11/C12]



Scheme S1 Schematic representation of the possible coordination modes of the ligand ‘tptz’



Scheme S2 [a] Availability and the nature of coronation pockets in tptz and [b] Schematic representation of steric constrain of the protonated ligand (Htptz^+) executed by the hydrogen atoms on the approach of second metal ion (M2) when it is already coordinated to the first metal ion (M1)



Scheme S3 Schematic representation of the synthesis of complex 1

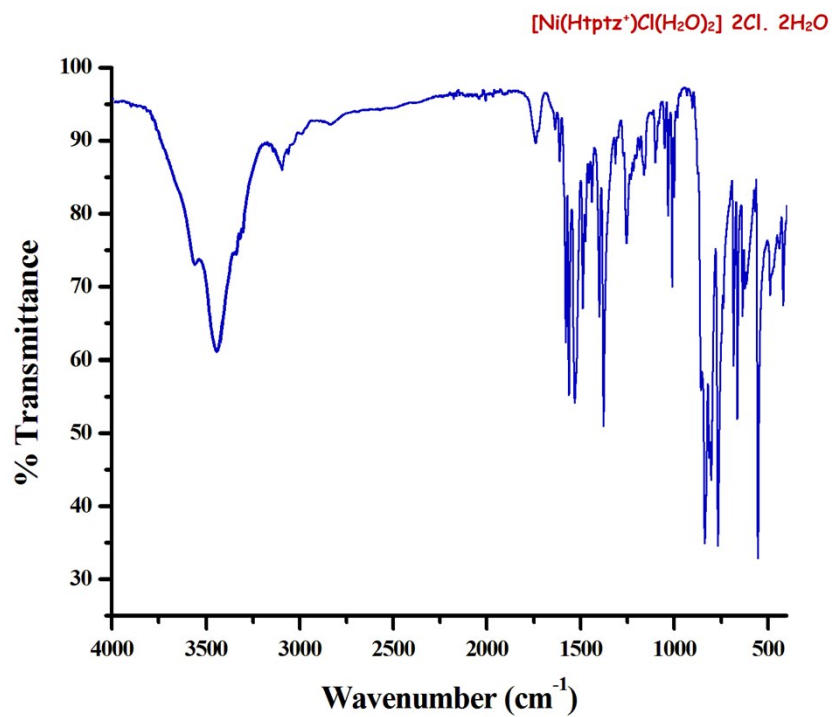


Fig. S1: IR spectrum for Complex 1

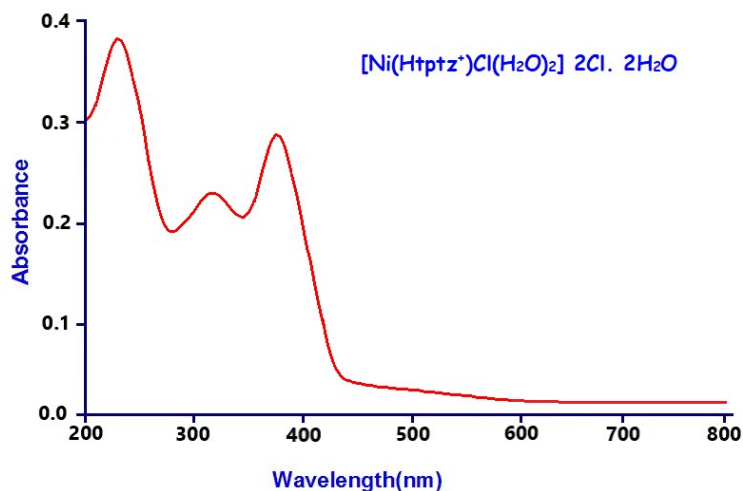


Fig. S2: UV-Visible spectrum for Complex **1**

The electronic absorption spectrum of **1** ($t_{2g}^6e_g^2$ system) has been recorded in methanol and it exhibits three bands at 233 nm, 311 nm and 379 nm. The intense absorption bands seen in the UV ($\lambda = 200\text{-}400$ nm) region are assigned to ligand-centered $\pi \rightarrow \pi^*$ and $n \rightarrow \pi^*$ transitions. The band at 379 nm became slightly broader may be assigned to LMCT. Unfortunately, the expected weak Laporte forbidden transitions in the visible region could not be detected even with concentrated solutions, might be lost in the low energy tail of the charge transfer transitions.¹

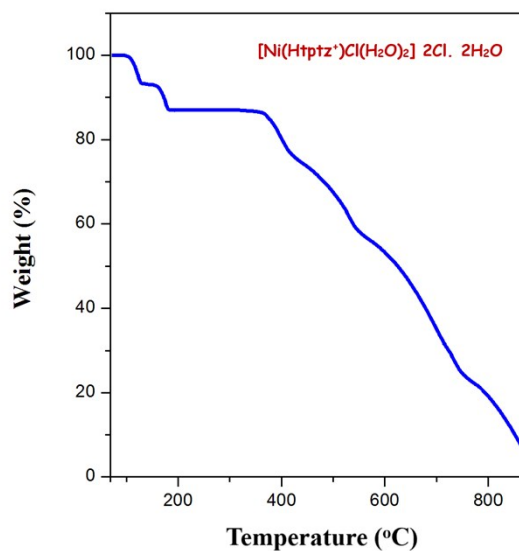


Fig. S3: TGA of Complex **1** measured under N₂ atmosphere.

